Electronic Supplementary Material (ESI) for Physical Chemistry Chemical Physics.

Supplementary Information

Time-resolved FTIR study on the structural switching of human galectin-1 by light-induced disulfide bond formation

Kunisato Kuroi[*ab], Mana Kamijo[b], Mutsuki Ueki[b], Yusuke Niwa[a], Hirotsugu Hiramatsu[cd], Takakazu Nakabayashi[*ab]

[a] *Graduate School of Pharmaceutical Sciences, Tohoku University, Sendai 980-8578, Japan*

[b] *Faculty of Pharmaceutical Sciences, Tohoku University, Sendai 980-8578, Japan*

[c] *Department of Applied Chemistry and Institute of Molecular Science, National Chiao Tung University, 1001, Ta-Hsueh Road, Hsinchu 30010, Taiwan*

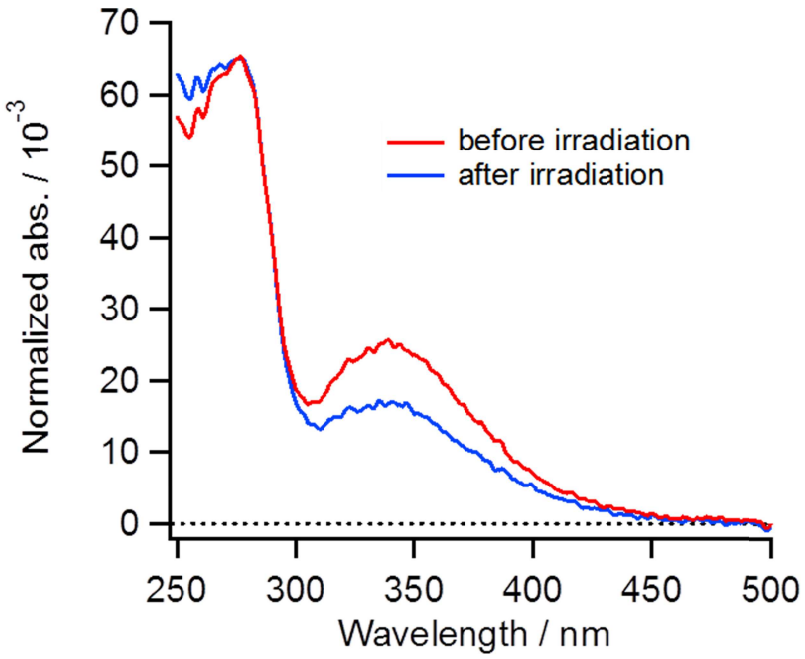

Fig. S1 UV-Vis spectra of SNO-hGal-1 before and after 5 min of photoirradiation with 355 nm light. Both spectra are normalised at ~280 nm due to Trp. The broad absorption at ~340 nm corresponds to the SNO group. The absorption of SNO reduced to one-third upon photoirradiation.

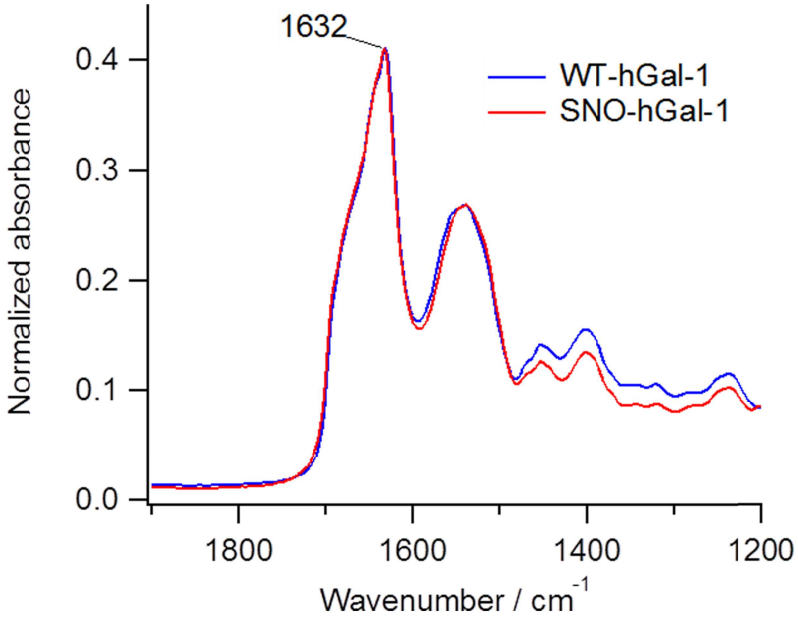

Fig. S2 IR spectra of SNO-hGal-1 and reduced WT-hGal-1 in the dried film state. Spectra are normalised at the amide I band at 1632 cm^{-1}.

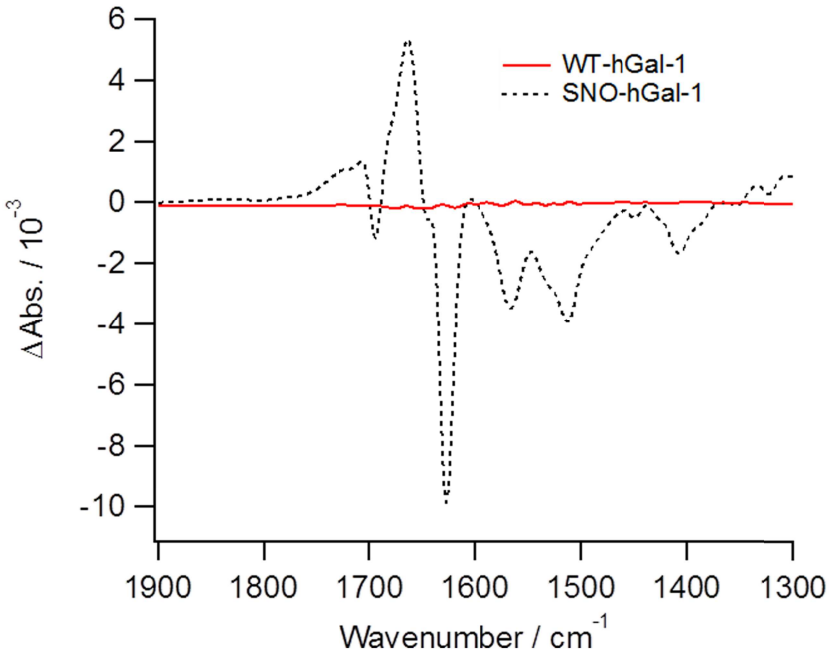

Fig. S3 Photo-induced IR difference (light-minus-dark) spectrum of WT-hGal-1 (red solid line) and SNO-hGal-1 (black dotted line). The photoirradiation wavelength was 355 nm. Only negligible changes were observed for WT-hGal-1.

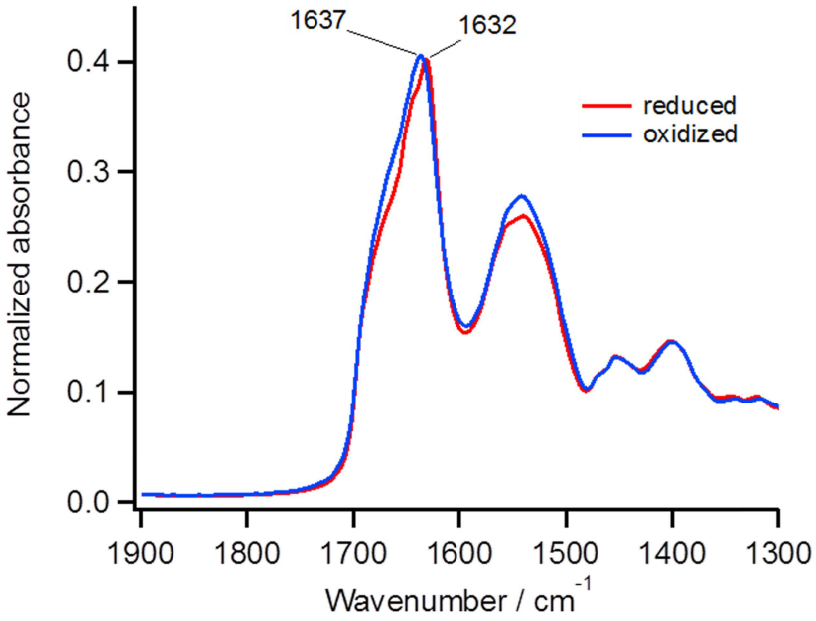

Fig. S4 IR spectra of reduced and oxidized WT-hGal-1 in a dried film state. Spectra are normalized at the amide I band.

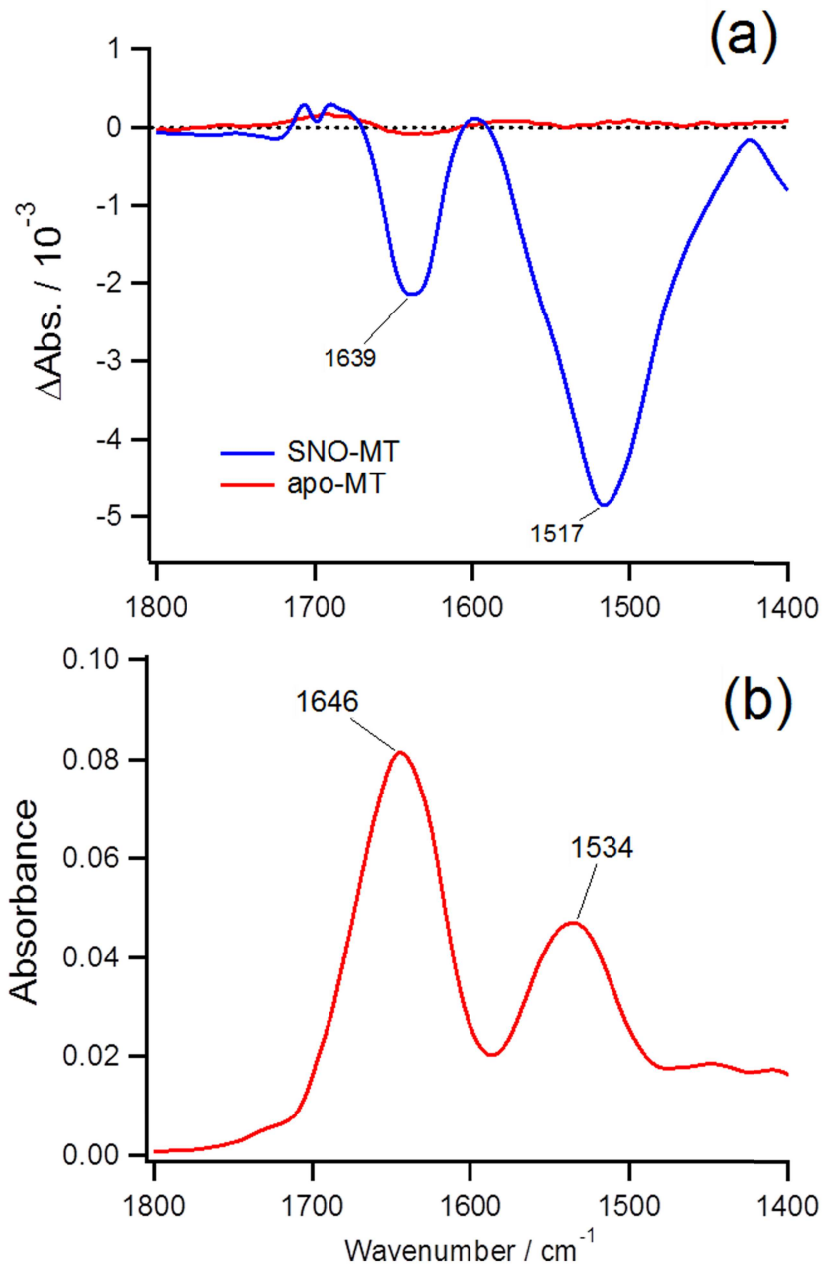

Fig. S5 (a) Photo-induced IR difference spectrum of *S*-nitrosylated metallothionein (SNO-MT) (blue line) and apo-MT (red line). The photoirradiation wavelength was 355 nm. (b) IR spectrum of SNO-MT in the dried film state.

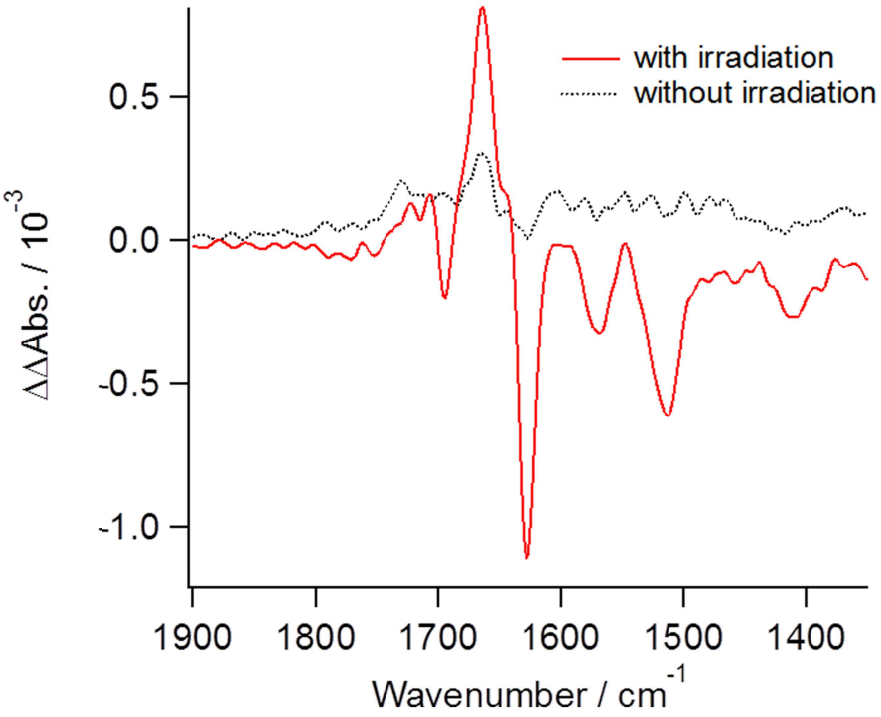

Fig. S6 Difference of the IR spectra of SNO-hGal-1 between the 0 and 45 min after irradiation of 355 nm light (red solid line) or without photo-irradiation (black dotted line).

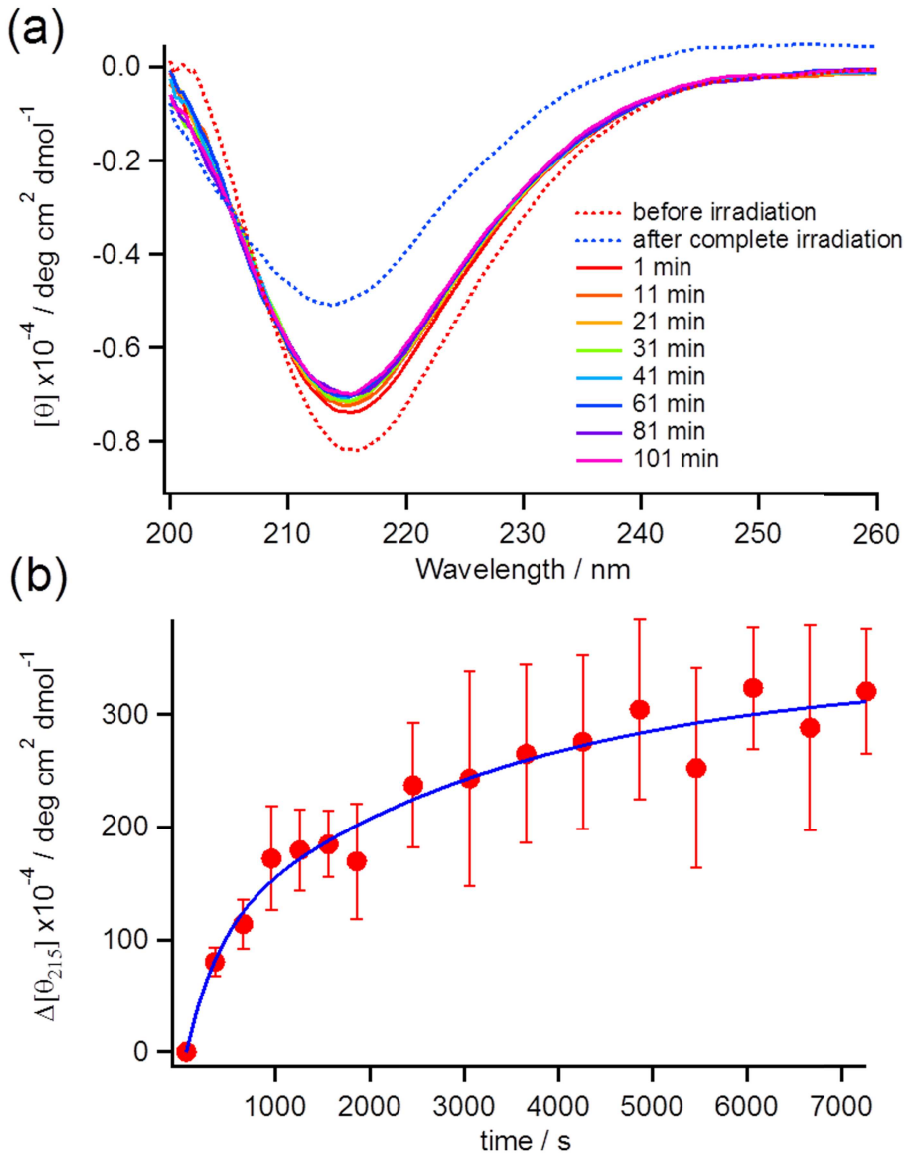

Fig. S7 (a) Time-resolved CD spectra of SNO-hGal-1 after irradiation of 355 nm light for 5 min (solid lines) in the solution state. The concentration of SNO-hGal-1 was 3.3 μM. Red and blue dotted lines are the CD spectra before and after 15 min of photoirradiation, respectively. Most of SNO-hGal-1 changed to the oxidised form after 15 min of photoirradiation. (b) Temporal profile of the CD intensity at 215 nm (θ_{215}) in (a). The difference (θ_{215} (at t min) minus θ_{215} (at 1 min)) is plotted. Blue solid line represents the fitting curve by a double-exponential function.

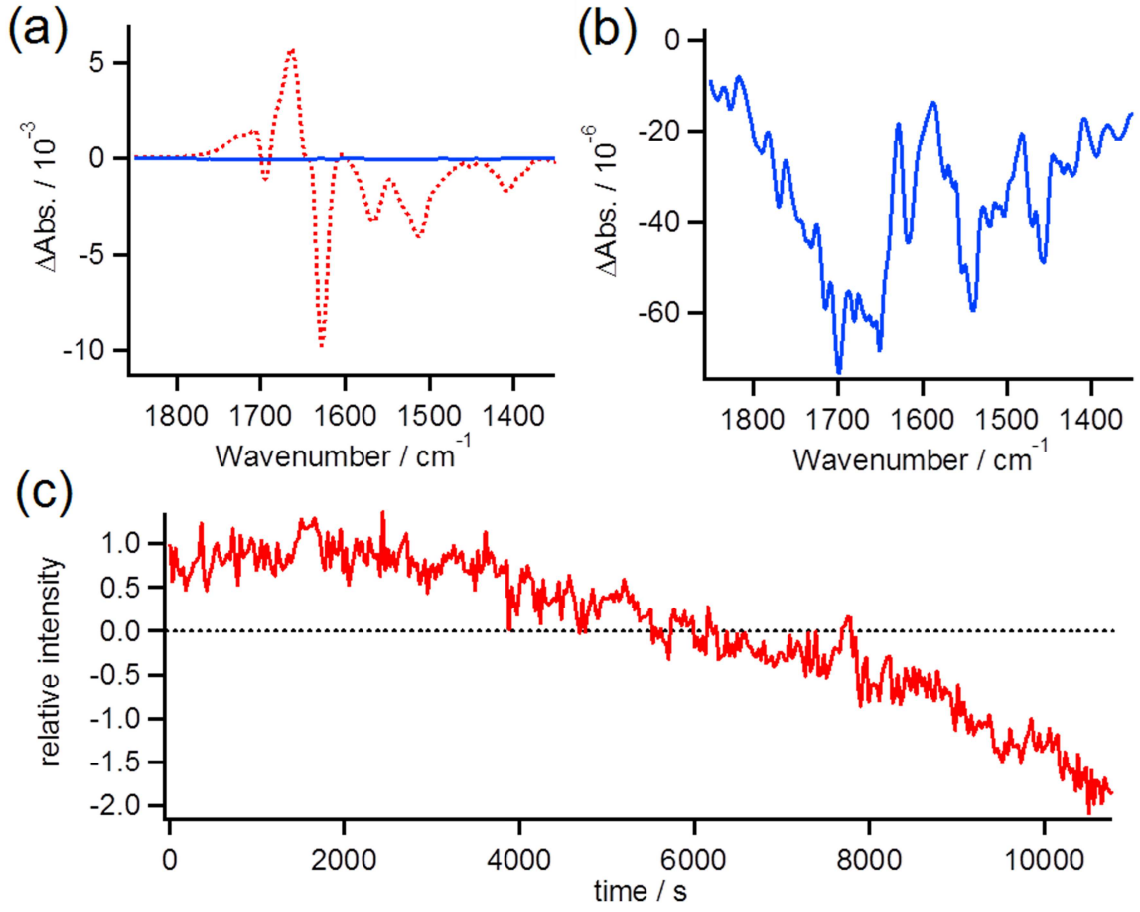

Fig. S8 Spectral ($W(\lambda)$) and temporal ($T(t)$) profiles extracted from the SVD analysis of the time-resolved IR spectra of SNO-hGal-1. (a) $S_V W(\lambda)$ of the first (red dotted line) and second (blue solid line) components. Note that the contribution of the second component is negligibly small. (b) Expanded figure of $S_V W(\lambda)$ of the second component. (c) Temporal intensity change relative to that at 0 min ($T(t)$) of the second component.

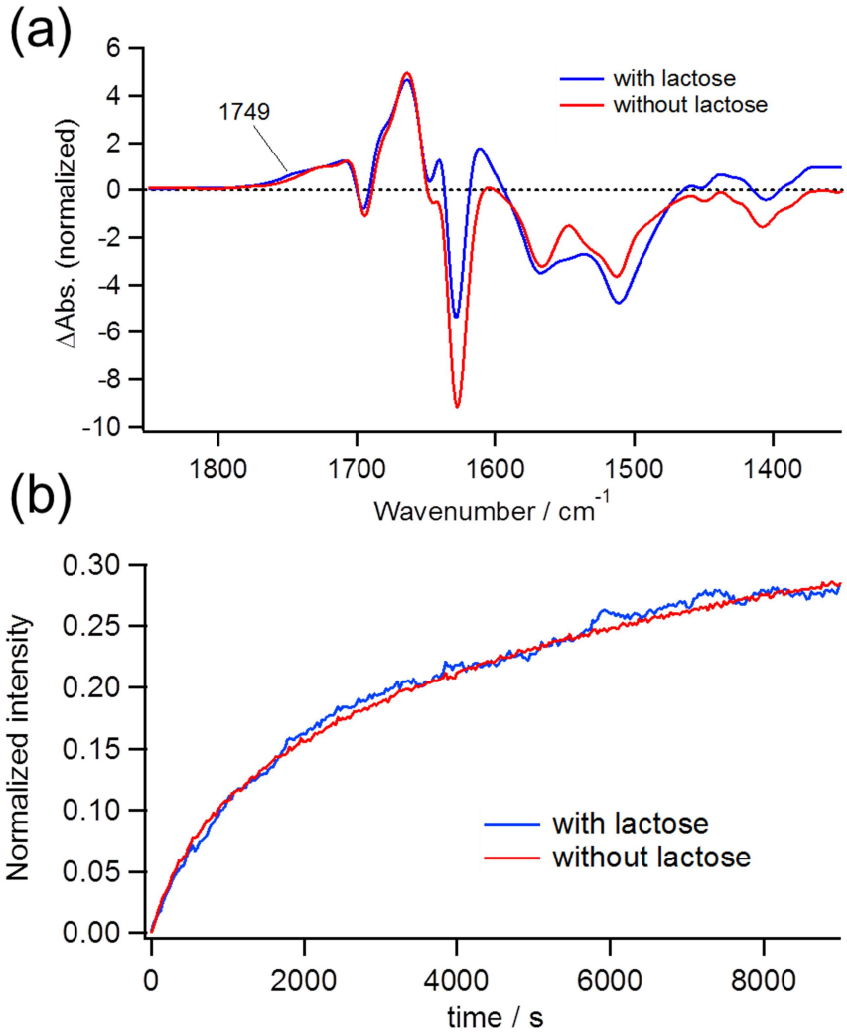

Fig. S9 (a) Photo-induced IR difference spectra of SNO-hGal-1 with (blue line) and without (red line) lactose. (b) Temporal profile relative to that at 0 min ($T(t)$) of the time-resolved IR of SNO-hGal-1 with (blue line) and without (red line) lactose from SVD analysis. In the figure, $T(t)$-1 is plotted and normalized between both of the conditions (with and without lactose) to compare temporal behaviours.

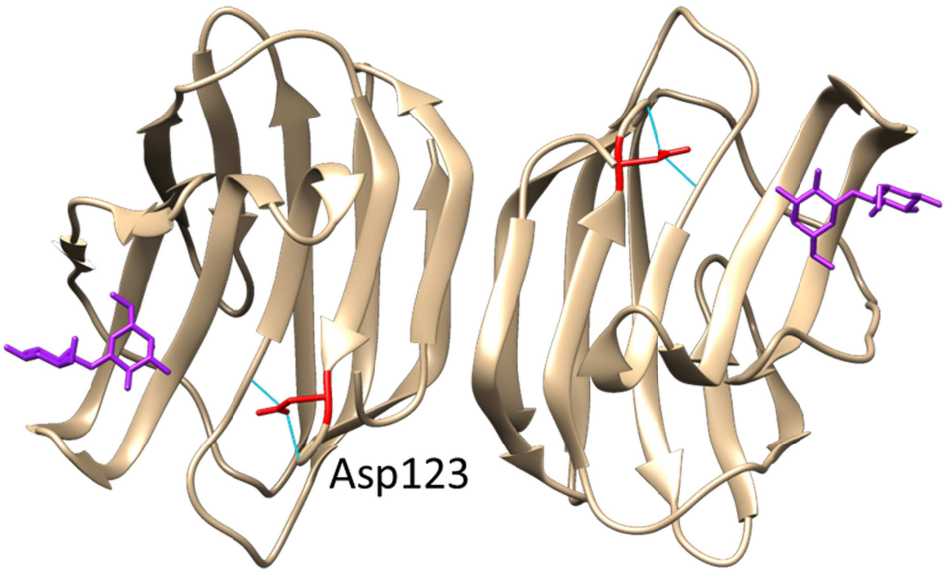

Fig. S10 Location of Asp123 in the hGal-1 dimer. Asp123 is shown as a red stick model, and its hydrogen bonds connecting adjacent loops are shown as blue solid lines. Lactose molecules are depicted as purple stick models.

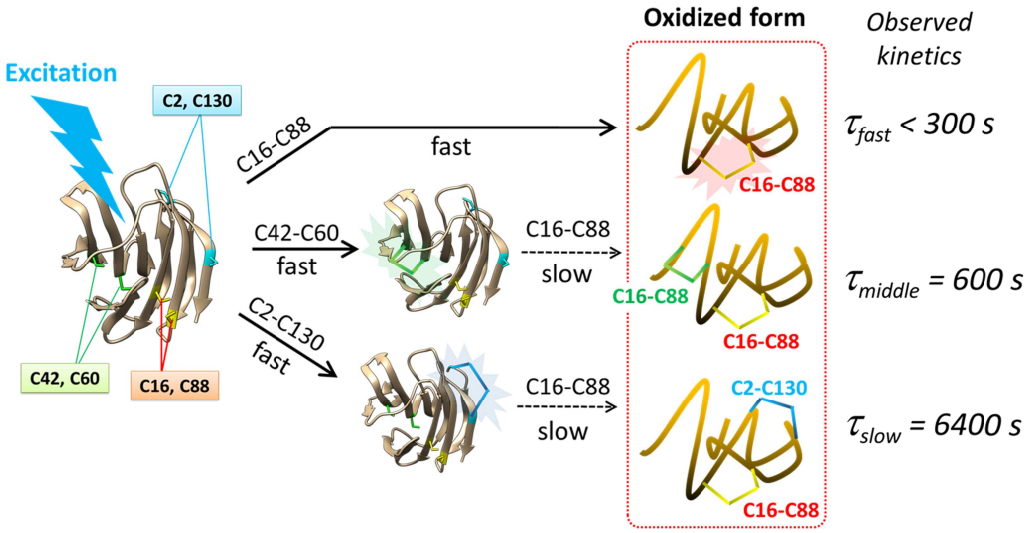

Fig. S11 Schematic figure of the proposed three reaction pathways of SNO-hGal-1 after the photo-induced disulfide formation in Cys16-Cys88, Cys-42-Cys60 and Cys2-Cys130, which are assignable to observed three kinetics (τ_{fast} < 300 s, τ_{middle} = 600 s, τ_{slow} = 6400 s). Three pairs of Cys16-Cys88, Cys42-Cys60, and Cys2-Cys130 are shown by yellow, green, and blue, respectively. In the right of the figure, oxidized structures of hGal-1 having different disulfide bonds are depicted. These oxidized forms of hGal-1 are all induced by the key disulfide bond of Cys16-Cys88.